

空间光学遥感器精密次镜调整机构设计及试验

武永见, 杨大伟, 孙 欣, 刘 涌, 胡永力

(北京空间机电研究所 先进光学遥感技术北京市重点实验室, 北京 100094)

摘要: 随着空间光学遥感器地面分辨率逐步提高, 长焦距、大口径相机成为重点研究方向。为了克服重力变化、复合材料变形等因素带来的天地不一致性的问题, 次镜调整成为校正光学遥感器离焦和主次镜相对位置变化的关键技术之一。将次镜柔性支撑、精密直线驱动与柔性铰链传动技术相结合, 设计了一套高精度次镜调整机构。首先介绍了该套机构的光机构成、工作原理及传动链路, 然后对超轻次镜、高精度直线致动、高精度调焦传动等设计分别进行了阐述, 最后介绍了力学环境试验后的调整精度测试情况。试验结果表明, 该套精密调整机构实测调整行程大于 $\pm 120 \mu\text{m}$, 轴向调整步距精度 $0.18 \mu\text{m}$ (3σ 值), 调整行程内次镜的最大平移误差为 $1.30 \mu\text{m}$, 最大倾斜误差为 $1.93''$, 具有调整范围宽、调整精度高的特点, 满足空间光学遥感器精密次镜调整的要求, 已成功在轨应用于北京三号 B 卫星 0.5 m 级高分辨率空间相机。

关键词: 大口径; 空间光学; 调整机构; 遥感器; 次镜; 柔性支撑

中图分类号: TH751 **文献标志码:** A **DOI:** 10.3788/IRLA20220635

0 引言

随着空间光学遥感器技术的不断进步和地面分辨率逐步提高, 长焦距、大口径空间相机成为未来航天光学遥感领域的重点研究方向^[1]。为了克服地面和在轨环境重力、材料变形等差异带来的天地不一致性的问题, 包括次镜调整在内的各种调焦技术成为校正光学遥感器离焦或主、次镜相对位置变化的主要手段之一^[2-5]。

国外在次镜及空间光学元件的调整方面已经积累有大量的理论和应用经验, 比如在哈勃望远镜、美国锁眼系列侦察卫星上成功应用的六自由度并联机构, 具有高精度、高承载能力以及高刚度的优势, 具备对光学系统中的次镜组件进行精密调整的能力^[6]。Aiala Artagoitia 等人设计了一种三自由度定位机构对 ECULID 望远镜的次镜进行精密调焦, 调整精度为 $3 \mu\text{m}$; Karig Koski 等人研制了一种新型调焦机构, 利用柔性铰链实现主反射镜的调焦, 调焦机构精度 $7.4 \mu\text{m}$ ^[7]。尽管次镜调焦技术在国外多个高分军用和商用遥感相机上均已经取得成功应用, 但由于该项技术是大口径空间光学遥感器的核心技术之一, 其详细

性能参数较难获取。国内的空间相机调焦技术路线偏于保守, 一般通过调节平面镜、三镜、中继透镜或焦平面进行调焦, 调整分辨率一般在 $10 \mu\text{m}$ 级^[8], 同时极少选取光学敏感度极高的次镜进行调整, 这也导致国内次镜调焦相关的理论研究偏多, 鲜见在轨应用。国内部分学者对六自由度调整机构做了较多的理论分析和工程研究, 但是六自由度调整机构同样具有结构及控制系统复杂、成本较高以及质量相对偏大的不足^[9-10]。单自由度高精度次镜调整机构同样具有高精度、高集成度以及高可靠性的优势, 更加适用于中小口径商业光学遥感器。马晓哲等人设计了一种应用于高分辨率多光谱空间相机的精密次镜调焦机构, 调焦范围为 $40 \mu\text{m}$, 调焦精度优于 $1 \mu\text{m}$ ^[11-12]。

文中针对某高分辨率相机次镜调整需求, 将高精度直线传动、柔性铰链传动与次镜柔性支撑相结合, 设计了一套高精度、高稳定性的次镜调整机构。介绍了该套机构的光机构成及调整原理, 对精密调整机构涉及的次镜柔性支撑、高精度直线致动、高精度调焦传动等分别进行了分析。调整机构光机产品的力学环境考核后的调整精度测试结果表明, 机构具有在大范围内实现亚微米级高精度调整的能力, 满足空间光

收稿日期: 2022-09-07; 修訂日期: 2022-11-17

作者简介: 武永见, 男, 高级工程师, 硕士, 主要从事空间光学遥感器光机结构设计方面的研究。

学遥感器在轨应用需求。

1 构成及原理

1.1 光机组成

次镜调整机构如图1所示,包括次镜组件(实现次镜支撑及其自由度约束)、调焦传动组件(实现高精度柔性铰链传动)以及直线传动组件(作为次镜调整机构输入,输出精密直线运动)。

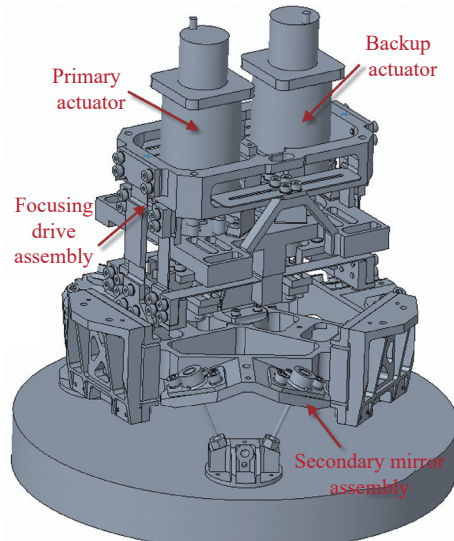


图1 次镜调整机构

Fig.1 Secondary mirror adjustment mechanism

1.2 工作原理

次镜调整机构的基本原理如图2所示,调整机构左右完全对称且具备主备份调焦能力,结构上包含次镜及导向铰链、柔性传动机构、主(备)份直线驱动器以及倾斜盘等几个部分。主(备)份直线传动组件具备优于 $2\text{ }\mu\text{m}$ 分辨率精密致动能力,假如A点向图2所示的下方运动 $1\text{ }\mu\text{m}$,B点会以P为支点向上运动 $0.2\text{ }\mu\text{m}$ (AP和BP长度比例为 $5:1$),从而带动“倾斜盘”以D为支点顺时针旋转,进而对称面上H点柔性变形片向上运动且位移量为C点的 $1/2$,从而驱动次镜发生 $0.1\text{ }\mu\text{m}$ 的精密轴向运动。

即次镜调整机构将直线传动组件的直线输出通过柔性铰链的变形转换为调焦传动组件顶端的“倾斜盘”运动,从而驱动次镜组件的高精度移动。次镜调整机构具有以下特点。

(1) 驱动机构冗余设计:驱动电机是调整机构设计的关键,采取驱动机构冗余设计以保证可靠性,主

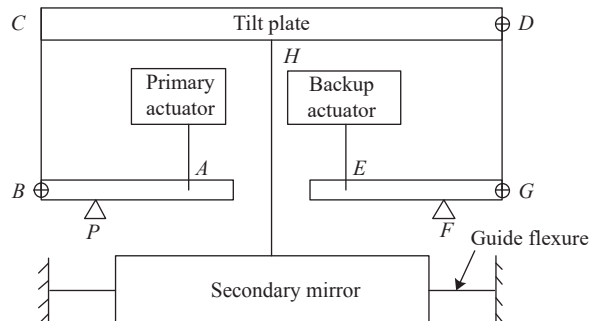


图2 次镜调整机构原理

Fig.2 Principle of the secondary mirror focusing mechanism

(备)份电机中的任何一个正常工作均可保证调整机构功能及性能;

(2) 采用柔性铰链传动:相比传统的齿轮减速具有冲击小、无磨损、传动平稳、可靠性高的优点,同时柔性铰链在微小位移范围的传动中具有较高的精度;

(3) 柔性导向铰链:通过柔性导向铰链的设计,使次镜及其组件在光轴方向具有一定柔性,而在其他方向上刚度较强,保证调焦过程中次镜的倾斜以及偏心在一定的误差范围内。

1.3 传动链路

次镜调整机构从步进电机输出旋转运动到次镜的高精度移动共经过三个环节减速,其中包含一次旋转运动到直线运动的转换,传动比分配如下。

环节一:步进电机配合行星齿轮减速器,减速比 $i_A=112.89:1$;

环节二:切口螺母旋转转换为螺纹传动导杆的直线运动,螺纹导程 $S=1.0\text{ mm}$;

环节三:柔性传动铰链构成减速比 $10:1$ 的差分减速杠杆,减速比 $i_B=10:1$ 。

步进电机步距角 $\gamma=1.8^\circ$,按上述传动关系,理论上次镜沿轴向的移动分辨率 d 按照公式(1)给出:

$$d = (\gamma/360^\circ) \times (1/i_A) \times S \times (1/i_B) \quad (1)$$

计算可知分辨率 d 为 4.4 nm ,次镜的移动步距取决于步进电机的控制,在轨调焦一般按照每 $128/64/32$ 步作为一个最小控制量,对应的次镜移动分辨率为 $128d/64d/32d=0.56\text{ }\mu\text{m}/0.28\text{ }\mu\text{m}/0.14\text{ }\mu\text{m}$ 。

2 设计与分析

2.1 超轻次镜组件

图3为次镜组件示意图,包括具有较高比刚度的

蜂窝夹芯式 ULE 次镜及支撑背板、Bipod 杆以及柔性导向铰链等。

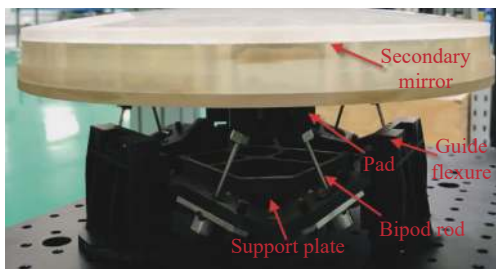


图 3 次镜组件的装调

Fig.3 Installation and adjustment of secondary mirror assembly

2.2 高精度直线致动

采用步进减速电机作为动力,如图 4 所示。通过滑动螺旋传动实现旋转运动转化为直线输出,具有结构紧凑、运转平稳、易于自锁的特点,通过预紧弹簧进行消间隙控制以确保传动精度和稳定性。

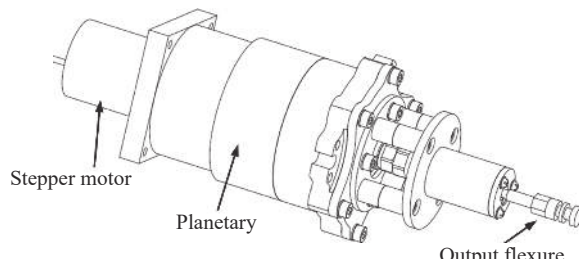


图 4 高精度直线致动组件

Fig.4 High precision linear actuator assembly

常用的螺旋传动包括滑动螺旋传动以及滚动螺旋传动,二者的对比如表 1 所示。

表 1 常用的螺旋传动对比

Tab.1 Comparison of common screw drives

	Sliding spiral drive	Rolling screw drive
Advantages	Simple structure and low cost; Easy to self-lock	Low friction and high transmission efficiency; No additional clearance elimination design required
Disadvantages	High friction and low transmission efficiency; Clearance elimination design is required	Complex structure and high cost; Need anti reversal design

2.3 高精度调焦传动

调焦传动组件是基于柔性变形原理设计的铰链

传动机构,可以实现图 2 所示的调焦功能,传动铰链具备 10 : 1 的传动比,为左右对称式构型。

2.4 精密次镜导向

次镜组件通过三处周向分布的柔性铰链实现次镜的精密导向,柔性铰链使次镜在沿光轴方向具有一定柔性的同时,限制次镜其他自由度。

2.5 位置遥测

调焦过程中为了探测次镜在调整机构工作时所处的绝对位置,直线传动组件末端采用直线差分传感器 LVDT(Linear Variable Differential Transformer) 反馈直线传动组件末端直线运动的绝对位置,构建闭环控制系统,如图 5 所示。

次镜调焦过程中,直线差分传感器组件中的差分传感器输入轴、差分传感器输出轴在差分传感器内腔滑动,通过数据采集设备即可测量得到直线传动组件的位置,差分传感器输出轴的位移等价于图 2 中 A 点(主份)或 E 点(备份)的绝对位置变化量,由于柔性传动铰链是设计状态为减速比 10 : 1 的差分减速杠杆,因此闭环控制时可直接通过差分传感器输出轴除以 10 得到次镜的位移。

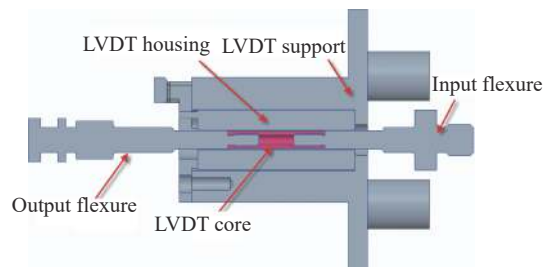


图 5 直线差分传感器

Fig.5 LVDT linear differential sensor assembly

2.6 真空防冷焊

空间防冷焊的方式包括运动副选用不同的材料、固体润滑以及油脂润滑等形式。次镜组件采用柔性铰链释放沿光轴方向的自由度,调焦传动组件通过柔性铰链的变形传递运动,无需采用防冷焊措施。对于直线致动组件涉及的步进电机、行星齿轮减速器涉及的轴承和齿轮副均采用表面镀覆 MoS₂ 固体润滑薄膜层防止冷焊效应的发生。

滑动螺旋副采用切口螺母与螺纹导杆配合的形式,选用青铜与超硬不锈钢两种不同的配合材料,啮

合段表面涂覆真空润滑脂进行防冷焊,通过调节切口螺母外预紧环实现螺纹消隙,如图 6 所示。



图 6 切口螺母于螺纹导杆配合

Fig.6 Split nut fits with threaded guide rod

3 试验与结果

3.1 试验状态

该套精密调整机构在完成力学试验后开展了调整精度试验,试验按照步进减速电机每次转 0.088° (对应的次镜理论步距 $8.858 \mu\text{m}$)进行调整,次镜的初始位置为零位,驱动次镜依次完成“零位、正极限位置、零位、负极限位置、零位”整个调整循环。

如图 7 所示,调整机构精度测试时次镜调整机构放置于三坐标平台,光轴竖直向上。首先通过三坐标采集次镜三杆上三处周向 120° 均布的共面凸台建立测量基准,然后采集次镜在每次调整步距下的外圆柱拟合圆心的平移变化,用于表征次镜偏心量。通过采集次镜背部平面与测量基准面之间距离及法线的变化计算次镜的绝对位置和倾斜量。

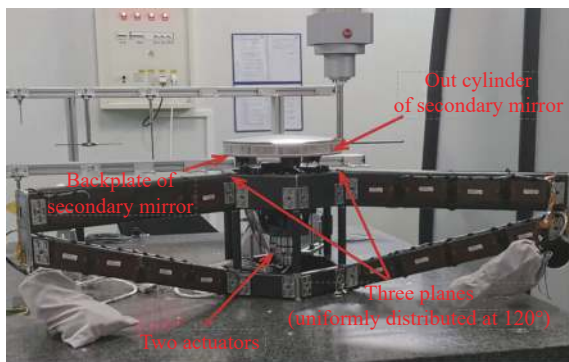


图 7 调整机构精度测试状态

Fig.7 Adjustment mechanism accuracy test

3.2 调整行程

如图 8 所示,实测次镜的调整行程为 $+128.6\sim-134.6 \mu\text{m}$,结果满足 $\geq \pm 120 \mu\text{m}$ 调整范围的要求,其中

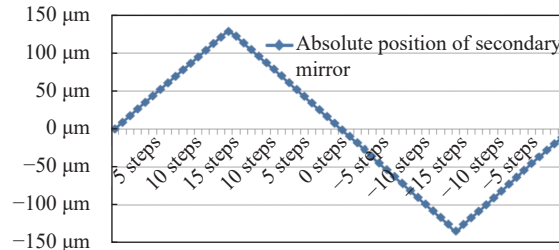


图 8 调整行程

Fig.8 Adjustment range

横坐标为步进减速电机的调整步数,纵坐标为次镜的绝对位置。

3.3 倾斜偏差

如图 9 所示,横坐标为次镜的绝对位置,纵坐标为次镜在各位置的倾斜。次镜在整个调整行程内的倾斜偏差总均方根最大值为 $1.93''$,满足总体要求的在调整行程内倾斜小于 $3''$ 的要求。

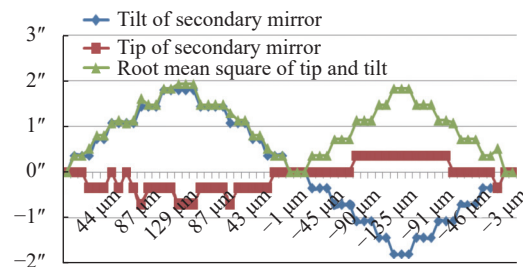


图 9 次镜的倾斜偏差

Fig.9 Inclination deviation of secondary mirror

3.4 次镜偏心量

如图 10 所示,横坐标为次镜的绝对位置,纵坐标为次镜在各位置的偏心量。可以看出次镜偏心量的总均方根最大值为 $1.33 \mu\text{m}$,满足总体要求小于 $5 \mu\text{m}$ 的要求。

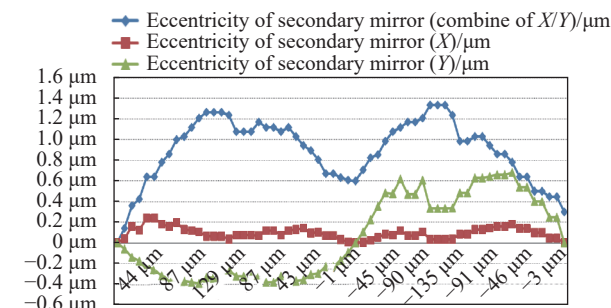


图 10 次镜的偏心量

Fig.10 Eccentricity of secondary mirror

3.5 步距精度

如图 11 所示, 横坐标为完成“零位、正极限位置、零位、负极限位置、零位”整个调整循环对应的步进减速电机调整步数, 纵坐标为每次调整对应的次镜实测步距。可以看出, 实测调整步距达到设计预期。

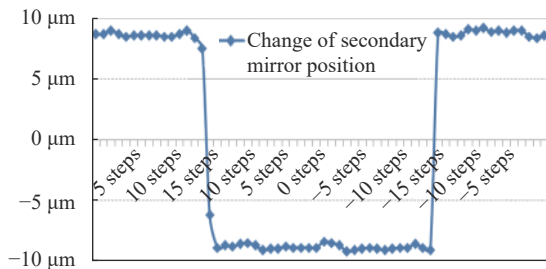


图 11 调整步距

Fig.11 Adjustment step of the secondary mirror

次镜调整机构的步距精度 (3σ 值) 按公式(2)给出, 定义为每次实测步距相对于标定步距的偏差, 取多次测量的标准偏差 RMS 的 3 倍。实测次镜步距为 $8.732 \mu\text{m}$, 步距精度 $AS_n(3\sigma)$ 为 $0.18 \mu\text{m}$ 。

$$AS_n = \sqrt{\frac{\sum_{i=1}^n (d_i - S_n \times n)^2}{n-1}} \times 3 \quad (2)$$

式中: S_n 为标定步距, 即通过测量得出的平均步距; i 为调节次数; n 为调节单位; AS_n 为调焦步距精度 3σ 值; d_i 为调节一个 n 单位时的实测调节距离。

4 结 论

文中针对高分辨率相机次镜调整机构高精度、高稳定性以及一体化设计的需求, 将次镜柔性支撑、精密直线驱动与柔性铰链传动技术相结合, 设计了一套精密次镜调整机构。介绍了该套机构的光机构成及调整原理, 对精密调整机构涉及的次镜柔性支撑、高精度直线致动、高精度调焦传动等分别进行了阐述。最后, 开展了调整机构力学试验后的调整精度测试。试验结果表明: 该套精密调整机构力学试验后的实测调整范围大于 $\pm 120 \mu\text{m}$, 轴向调整步距精度为 $0.18 \mu\text{m}$ (3σ 值), 调整行程内次镜的平移量为 $1.30 \mu\text{m}$, 最大倾斜量为 $1.93''$, 具有调整范围宽、调整精度高的特点, 满足空间光学遥感器精密次镜调整的要求, 成功取得在轨应用。

参考文献:

- [1] Qi Guang, Xu Yanjun, Liu Bingqiang. Lightweight structure design for SiC/AI supporting plate of space mirror [J]. *Infrared and Laser Engineering*, 2014, 43(7): 2214-2218. (in Chinese)
- [2] Tan Shuang, Liang Fengchao, Yan Nanxing, et al. Study of the envelope space determination algorithm of the stewart platform in the secondary mirror adjustment [J]. *Spacecraft Recovery & Remote Sensing*, 2021, 42(1): 108-114. (in Chinese)
- [3] Wei Xin, He Hongtao, Wang Jianyong, et al. A measurement method of parallel accuracy between the motion direction of the focusing mechanism and the optical axis [J]. *Spacecraft Recovery & Remote Sensing*, 2019, 40(5): 67-74. (in Chinese)
- [4] Liu Yuzhe, Zhang Xinyu, Zhang Qun, et al. Performance evaluation and parameters optimization of space telescope secondary mirror adjusting mechanism [J]. *Infrared and Laser Engineering*, 2019, 48(12): 1214004. (in Chinese)
- [5] Tan Wei, Wang Dianzhong, He Hongyan, et al. Research on high accurate refocusing method of GF-7 Camera [J]. *Spacecraft Recovery & Remote Sensing*, 2020, 41(2): 78-86. (in Chinese)
- [6] Boian R F, Bouzit M, Burdea G C, et al. Dual Stewart platform mobility simulator [C]//Engineering in Medicine and Biology Society, 2004(2): 4848-4851.
- [7] Jiang Ziqing, Jia Jianjun. Development of focusing mechanism for space camera [J]. *Optics and Precision Engineering*, 2018, 26(12): 2956-2962. (in Chinese)
- [8] Wang Kai, Yan Yong, Xu Minglin, et al. Design and experiment of precision focusing mechanism of space remote sensing camera with lightweight and miniaturization [J]. *Infrared and Laser Engineering*, 2018, 47(12): 1218004. (in Chinese)
- [9] Zhao Hongchao, Zhang Jingxu, Yu Xiaobo, et al. Design and optimization of stewart platform in TMT tertiary mirror system [J]. *Infrared and Laser Engineering*, 2012, 41(12): 3336-3341. (in Chinese)
- [10] Han Chunyang, Xu Zhenbang, Wu Qingwen, et al. Optimization design and error distribution for secondary mirror adjusting mechanism of large optical payload [J]. *Optics and Precision Engineering*, 2016, 24(5): 1093-1103. (in Chinese)
- [11] Ma Xiaozhe, Li Chuang, Cheng Penghui, et al. A focusing mechanism based on flexible hinges for space telescope [C]// Pacific Rim Laser Damage 2019: Optical Materials for High Power Lasers, 2019.
- [12] Ma Xiaozhe. Design and analysis of focusing mechanism for secondary mirror of high resolution space camera [D]. Xi'an: Xi'an Institute of Optics Precision Mechanics, Chinese Academy of Sciences, 2020. (in Chinese)

Design and test of precision secondary mirror adjustment mechanism for space optical remote sensor

Wu Yongjian, Yang Dawei, Sun Xin, Liu Yong, Hu Yongli

(Beijing Key Laboratory of Advanced Optical Remote Sensing Technology, Beijing Institute of Mechanics & Electricity, Beijing 100094, China)

Abstract:

Objective Vertical assembly and adjustment is one of the key technologies of long focal length and large aperture space camera. In order to overcome the inconsistency between the on-orbit and the ground caused by gravity change, material deformation and other factors, the secondary mirror adjustment has become one of the key technologies to correct the defocus of the optical remote sensor and the relative position change of the primary mirror and the secondary mirror. Precision secondary mirror adjustment technology has been widely used in high-resolution space optical remote sensors. For example, Stewart platform 6-DOF parallel mechanism, which has been successfully applied in Hubble telescope and reconnaissance camera, has the advantages of high accuracy, high bearing capacity and high rigidity, and has the ability to precisely adjust the secondary mirror components in the optical system. Many theoretical analysis and engineering research have been done on the 6-DOF adjustment mechanism in China, but the 6-DOF adjustment mechanism also has the disadvantages of complex structure and control system, high cost and relatively large weight. Therefore, it is necessary to develop a single-degree-of-freedom secondary mirror adjustment mechanism with high accuracy, high integration and high reliability to solve the inconsistency between heaven and earth faced by the current high-resolution space optical remote sensor.

Methods In order to meet the secondary mirror adjustment requirements of a high-resolution camera, a high-precision and high-stability secondary mirror adjustment mechanism combining precision linear transmission, flexible transmission and flexible support technology is built in this paper (Fig.1). The linear transmission device (Fig.4) adopts the redundancy design of one main and one standby, and has precision position telemetry capability. The flexible transmission hinge with transmission ratio of 10 : 1 is used for motion transmission. Compared with the traditional gear reducer, it has the advantages of small impact, no wear, stable transmission, and high reliability. At the same time, the flexible hinge has the advantages of high-precision transmission in the range of small displacement. The secondary mirror uses bipod flexible support to design unloading force thermal deformation, and ensures its flexibility along the optical axis direction (focusing direction) through three pairs of 120° flexible guide hinges.

Results and Discussions This set of precision adjustment mechanism has carried out adjustment precision test after completing the mechanical environment assessment. The test is carried out according to 0.088° rotation of step motor (corresponding theoretical step distance of secondary mirror 8.858 μm). The initial position of the secondary mirror is zero. The secondary mirror is driven to complete the whole adjustment cycle of "zero position→positive limit position→zero position→negative limit position→zero position". The adjustment accuracy test results after the mechanical environment assessment of the optical and mechanical products of the adjustment mechanism show that the mechanism has the ability to achieve high-precision adjustment in a large

range (Fig.8-11), and meets the requirements of the on-orbit application of space optical remote sensor.

Conclusions In this paper, a set of high-precision secondary mirror adjustment mechanism is designed by combining the flexible support, precision linear drive and flexible hinge transmission technology of the second mirror. This paper first introduces the optical and mechanical structure, working principle and transmission link of the mechanism, then describes the design of ultra-light secondary mirror assembly, high-precision linear actuation and high-precision focusing transmission, and finally introduces the adjustment accuracy test after the vibration test. The test results show that the measured adjustment stroke of the set of precision adjustment mechanism is more than $\pm 120 \mu\text{m}$, the axial adjustment step precision is $0.18 \mu\text{m}$, the maximum translation error of the secondary mirror within the adjustment stroke is $1.3 \mu\text{m}$, and the maximum tilt error is $1.9''$. It has the characteristics of wide adjustment range and high adjustment accuracy, and meets the requirements of the precision secondary mirror adjustment of the space optical remote sensor.

Key words: large aperture; space optics; adjustment mechanism; remote sensor; secondary mirror; flexible support